DEVELOPMENT OF A HIGH-THROUGHPUT MICROSPHERE SYSTEM FOR ANNEALED HYDROGELS

An Undergraduate Research Scholars Thesis

by

OMAR WYMAN

Submitted to the Undergraduate Research Scholars program
Texas A&M University
in partial fulfillment of the requirements for the designation as an

UNDERGRADUATE RESEARCH SCHOLAR

Approved by
Research Advisor: Dr. Daniel Alge

May 2016

Major: Biomedical Engineering

TABLE OF CONTENTS

ABSTRACT

Development of a High-Throughput Microsphere System for Annealed Hydrogels

Omar Wyman
Department of Biomedical Engineering
Texas A&M University

Research Advisor: Dr. Daniel Alge
Department of Biomedical Engineering

Poly(ethylene glycol) (PEG) gels are step-growth hydrogel networks that can be formed using thiol-ene polymerization. Four-arm PEG monomers can be functionalized with norbornene and then crosslinked with matrix metalloproteinase (MMP) degradable sequences. Current techniques to understanding angiogenesis involves using type I collagen which can be modified with various angiogenic factors to study different aspects of angiogenesis. However, the coupling of bulk and ligand densities prevents us from studying the effect of varying densities on cell invasion. This can be overcome by using a submerged electrospray to generate microspheres, which utilizes high voltage to overcome surface tension and results in the formation of droplets. The purpose of this proposal is to develop and characterize a microsphere system capable of accelerated wound healing by means of invasion depth manipulation via ligand and bulk density variation, as well as by means of porosity manipulation via submerged electrospraying droplet generation.

CHAPTER I

INTRODUCTION

Click chemistry is highly versatile and can be used to generate hydrogels of various densities and properties. Click chemistry reactions are high yielding, stereospecific, simple to preform and can be conducted in easily removable or benign solvents [1]. Unlike Michael-type reactions which occur under alkaline conditions and can lead to off-stoichiometric reaction of monomers [2], thiol-ene polymerization occurs at neutral pH and can be controlled both spatially and temporally. Covalently crosslinked poly(ethylene glycol) (PEG) gels are step-growth hydrogel networks that can be formed using thiol-ene polymerization [3]. These scaffolds are bio-inert and have no inherent biological activity [4], but can be modified with biochemical cues to assist with cell adhesion and invasion [5].

Cell-degradable hydrogels can be created under cytocompatible conditions by a radical-mediated step-growth reaction between norbornene and thiols [1]. Four-arm PEG monomers can be functionalized with norbornene and then crosslinked with matrix metalloproteinase (MMP) degradable sequences conjugated with cysteine [1], [6], [7]. Hydrogel networks crosslinked with MMP degradable sequences can also have cell-adhesive peptides incorporated into the network to allow cell spreading and attachment [1], [7]. These resulting scaffolds are cell-adhesive, cell-degradable, and be spatially and temporally controlled at a neutral pH.

Angiogenesis requires endothelial cells to undergo considerable changes when forming a new sprout [8]. Type I collagen is the most abundant protein in the human body [9], and has been

used in various types of invasion assays to study angiogenesis [10]. Current techniques to understanding this complicated process involves using 3D matrixes of type I collagen [11] which can be modified with various angiogenic factors to study different aspects of angiogenesis, such as cell-cell and cell-matrix interactions [12] [13]. Type I collagen has MMP-degradable and cell adhesive sites which interact with the endothelial cells and is coupled with bulk density. Since poly(ethylene-glycol) is bio-inert, MMP-degradable ligands and cell adhesive sites must be added in order to interact with the cell, thus allowing the control of the ligand density while maintaining similar bulk density.

Particle generation using microfluidic technology is an efficient, precise method for creating monodisperse particles, but can be costly to manufacture. Griffin *et al.* have shown that it is feasible to generate hydrogels using a microfluidic microsphere system that has accelerated wound healing when compared to nonporous gels [14]. Fabrication of hydrogel microspheres requires a droplet generation step and an appropriate gelation mechanism. Both processes must be cytocompatible in order to be useful. PEG hydrogels generated using thiol-ene polymerization can be used for temporal and spatial control over the gelation process at a neutral pH.

Unlike microfluidic approaches to particle generation, electrospraying has been shown to produce monodisperse particles with fast results at a higher yield when compared to microfluidic methods. Submerged electrospray [15], [16] utilizes high voltage to overcome surface tension of a fluid meniscus that results in the formation of droplets. This technique has been used by Young *et al.* for cell encapsulation and has the potential to create a high-throughput microsphere system [17]. Therefore the purpose of this proposal is to develop and characterize a microsphere system

capable of accelerated wound healing by means of invasion depth manipulation via ligand and bulk density variation, as well as by means of porosity manipulation via submerged electrospraying droplet generation.

CHAPTER II

MATERIALS AND METHODS

Macromer synthesis

Norbornene acid was conjugated to 4-arm PEG-hydroxyl to create 4-arm PEG-norbornene. In brief, this occurs through the addition of norbornene acid to the PEG-OH by symmetric anhydride *N*,*N*'-dicyclohexylcarbodiimide (DCC) coupling. Norbornene acid was dissolved in dichloromethane and reacted with DCC to couple the norbornenes. This was transferred anhydrously to a second reaction flask. The second reaction flask contained 20 kDa 4-arm PEG-OH dissolved in DCM, 4-(dimethylamino)pyridine and pyridine, and was stirred overnight. The urea by-product was filtered using a glass-fritted funnel. The filtrate was then washed in order to remove unreacted norbornenes. The final product was precipitated and washed with ice-cold diethyl ether. Proton nuclear magnetic resonance (^{1}H-NMR) was used to characterize the purity and functionality of the product.

Synthesis of the peptide sequences KCGPQG↓IWGQCK, and CRGDS was completed on a peptide synthesizer using solid-phase peptide reagents with fluorenylmethoxycarbonyl (Fmoc) chemistry on a Rink-amide resin. Peptides were cleaved from the resin and purified using reverse-phase high-performance liquid chromatography, and the molecular weights were confirmed by mass spectrometry.

Electrospray apparatus

A syringe pump held a 12 mL syringe containing the PEG macromer solution which was connected by Tygon tubing to a blunt end stainless steel 22G needle (inner diameter = 0.4 mm, outer diameter = 0.7 mm). A high DC voltage (0–30 kV) was applied to the needle from a high voltage power supply, and the earth electrode was a copper ring (20 mm diameter) suspended below the tip of the needle. The needle and ring were suspended in a 50 mL polypropylene centrifuge tube containing either a

solution of 35 mL of light mineral oil with 0.5 wt% Span 80 or hexanes with 0.5 wt% Span 80 as a surfactant.

Microsphere generation

For a given experiment, the syringe pump would be turned on to a prescribed flow rate, and then the voltage immediately applied. The system dispensed approximately 150 µL of polymer solution, then the voltage was removed and the flow rate turned off. While the droplets were forming, the system was then irradiated with UV light 3 min at an intensity of 10 mW/cm^2. Microspheres were isolated from the oil by adding PBS to the centrifuge tube and centrifuging at 4,400 rpm for 3 min. The oil was then aspirated and the pellet of beads in PBS was collected by pipette and resuspended in PBS. This washing step was repeated twice.

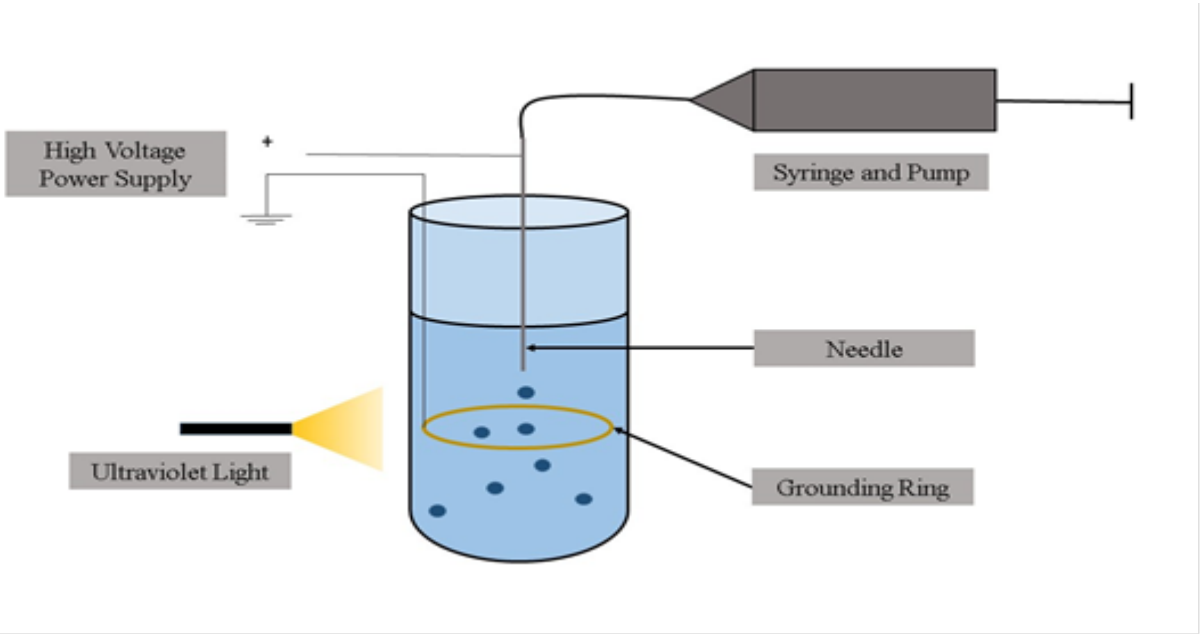

Figure 1. Submerged electrospray apparatus.

Annealed hydrogel formation

Previously synthesized microspheres are swelled to equilibrium size in PBS and pelleted through centrifugation. A solution of bifunctional PEG-NB, additional KCGPQG↓IWGQCK peptide linker, LAP

and PBS are then added to the microspheres. This new solution is then pipetted into a 1 mL syringe tip and photopolymerized for 3 minutes at 10 mW/cm^2.

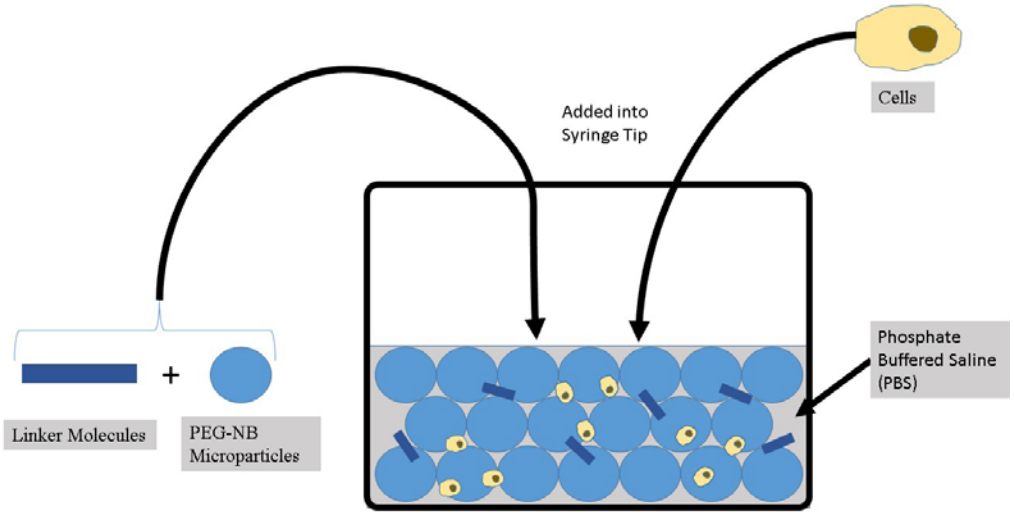

Figure 2. Annealed microsphere gel formation

Hydrogel generation

Bulk hydrogels were generated at various thiol-ene ratios. Briefly, four-arm PEG-NB, LAP, CRGDS adhesive ligand, KCGPQG↓IWGQCK peptide linker, and PBS was added into a microtube. The solution was then pipetted into a 1 mL syringe tip in 30 µL increments and polymerized for 3 minutes at 10 mW/cm^2.

Hydrogel characterization

Microspheres were imaged by optical microscopy for morphology and size. The compressive mechanical properties of the microspheres and resulting gels were determined at equilibrium swelling by uniaxial compression between smooth, parallel flat plates on a rheometer with a 1 N load cell. The modulus was determined from the load–distance data by Hertz theory. Annealed microspheres were compared to traditional bulk PEG-NB hydrogels of various thiol-ene ratios (0.65:1, 0.725:1, 0.85:1).

Cell invasion

Human umbilical vein endothelial cells (HUVECs) were cultured in Dulbecco's Minimum Essential Media (DMEM) supplemented with fetal bovine serum. When required for experiments, cells were trypsinized and resuspended in endothelial growth medium. PEG-NB microspheres (100 μm diameter) were generated as described above. Annealed microspheres were generated and allowed to equilibrate in endothelial cell culture media overnight. Resuspended cells ($1x10^6$ cells/mL) were then pipetted (30 μL) onto the surface of the gel and placed into the incubator for twenty minutes. Additional cell culture media was then added into the wells. The cellular invasion depth was then quantified using two-photon microscopy after seven hours of incubation.

CHAPTER III

RESULTS AND DISCUSSION

Microsphere characterization

To quantify the effects of flow rate and voltage on microsphere size, the microspheres were generated under four independent flow rates and three different voltages (Figure 3). Based on this data, within a given flow rate, an increase in voltage decreases the polydispersity of the microsphere size by decreasing the mean size of the particles. This concurs with previous research in the topic, as the Taylor cone that is formed from a combination the flow rate and the electric potential gradient has a strong effect on the microsphere formation. However, if the gradient opposes the surface tension and flow rate too strongly, the Taylor cone will not form completely and will become unstable leading to an increased range in microsphere sizes. This is evident by the increase in the standard deviation of the particles generated at 300 uL/min at 7 kV and 500 uL/min at 7 kV. By modifying previous mathematical models generated to predict the resulting sphere diameter with the information gained, we can generate a fairly robust model that can predict the mean particle diameter from the flow rate and voltage (Appendix A).

As the flow rate is increased, there is a drastic change in particle size and polydispersity. The combined effects of the electric potential gradient and flow rate counteract each other in determining the particle size, which allows for a variety of combinations which will lead to similar microspheres. However, we limit the combinations by requiring laminar flow of the solution. This is the fundamental requirement of the submerged electrospray system which will define the overall polydispersity of the microspheres generated.

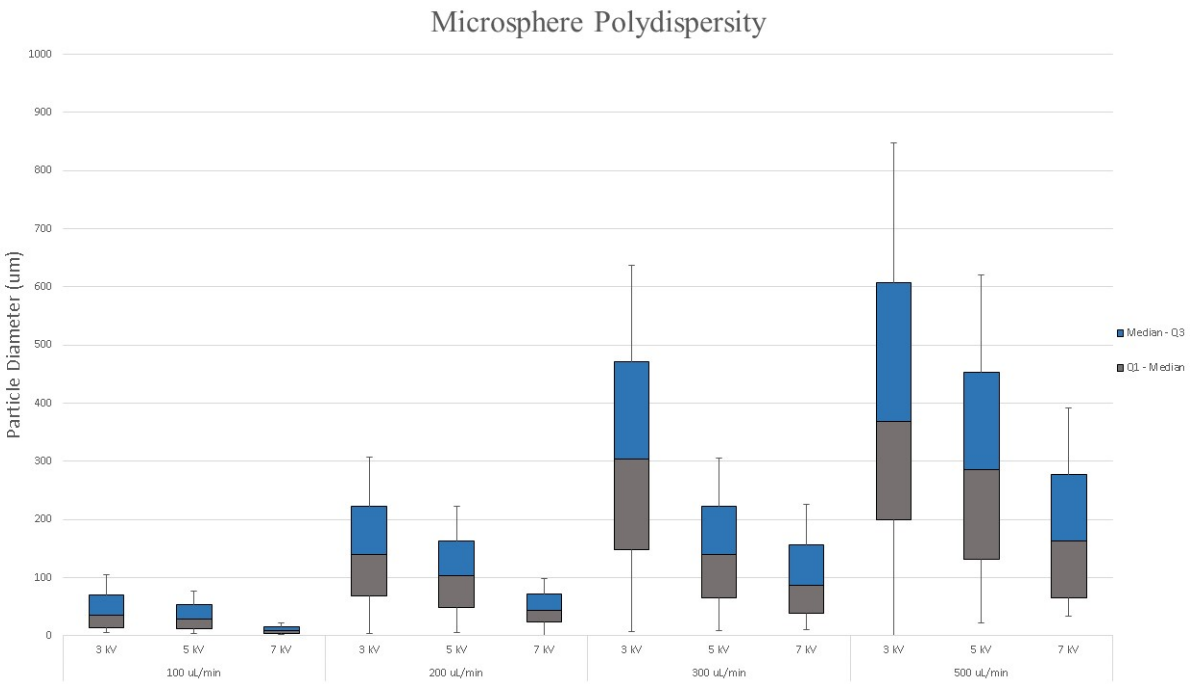

Figure 3: Microsphere polydispersity is dependent on flow rate and voltage. Relationship between the flow rate and voltage can control the polydispersity of the microspheres for a given diameter.

Annealed microsphere gels

The tissue engineering paradigm consists of three main components: biochemical cues, tissue scaffold, and cells. The biochemical cues and tissue scaffold can be controlled to shape cellular differentiation and phenotype, which can enable proper cell proliferation. A well understood component of these interactions is the cell-matrix relationship. The tissue scaffold stiffness greatly impacts the cellular phenotype, and thus, quantifying this aspect of the annealed hydrogels is an important step to understanding the potential of this system. The annealed microsphere system differs from traditional hydrogels in that there is the potential to control the microsphere stiffness by varying the microsphere size. This provides another layer of control for this system and can potentially improve upon existing hydrogels (Figure 4).

Graphs of Annealed Microspheres Diameter and Bulk Hydrogel Thiol-ene Ratios against Storage Modulus

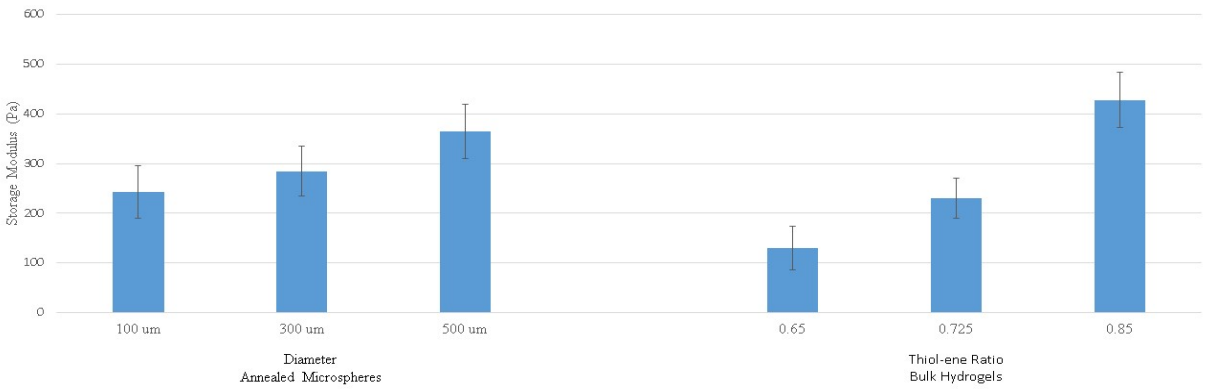

	100 um	300 um	500 um
Mean Storage Modulus (Pa)	243.2	284.9	364.9
Standard Deviation (Pa)	90.4	95.1	100

	0.65:1 thiol-ene	0.725:1 thiol-ene	0.85:1 thiol-ene
Mean Storage Modulus (Pa)	54.7	102	428
Standard Deviation (Pa)	13.9	17.7	39.3

Figure 4. Gel stiffness can be varied by changing sphere diameter instead of thiol-ene ratio. Here, annealed microspheres generated with a 0.75:1 thiol-ene ratio at various sizes are compared to bulk hydrogels of various thiol-ene ratios.

As the microsphere size increases, the annealed microsphere stiffness increases, since the majority of the gel strength lies within the microspheres. This is due to the increase in crosslink density within the larger particles, which increases the bulk storage modulus of the gel. However, compared to traditional hydrogels of the same composition, the storage modulus of the annealed microspheres are half as stiff. Crosslinking between particles does not generate a second scaffold that encapsulates the particles. Bright field images at 10x and 20x show that the microspheres are crosslinked together into a matrix, and that a secondary gel doesn't form around the microspheres (Figure 5).

The resulting stiffness of the annealed gels can also be compared to the resultant porosity (Figure 6). By assuming a perfectly packed mold, the spaces between spheres can be estimated as prisms. In this case, porosity can be defined as the empty volume within the gel with respect to the total polymer volume in

the gel. Since each annealed microsphere gel was made from the same amount of volume, the number of spheres in the gel changes as the diameter changes.

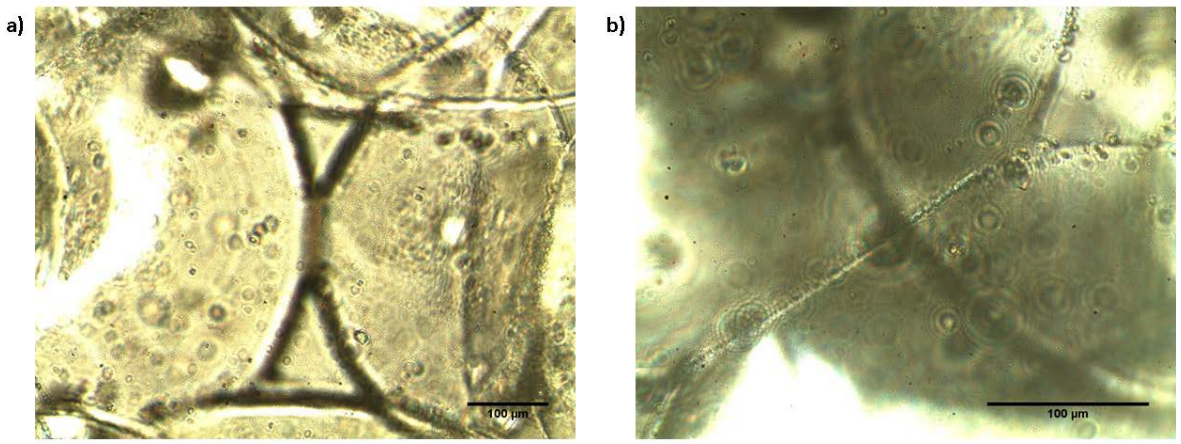

Figure 5. Microspheres anneal together at surface interface. a) Brightfield image at 10x showing microsphere connection and pores. b) Brightfield image at 20x showing intersection region of the microsphere.

From this, a new relationship is formed between the stiffness of the gel, number of particles within the gel, and the storage modulus. As the sphere size is increased, the porosity and number of spheres within the gel decreases but the overall stiffness of the gel increases.

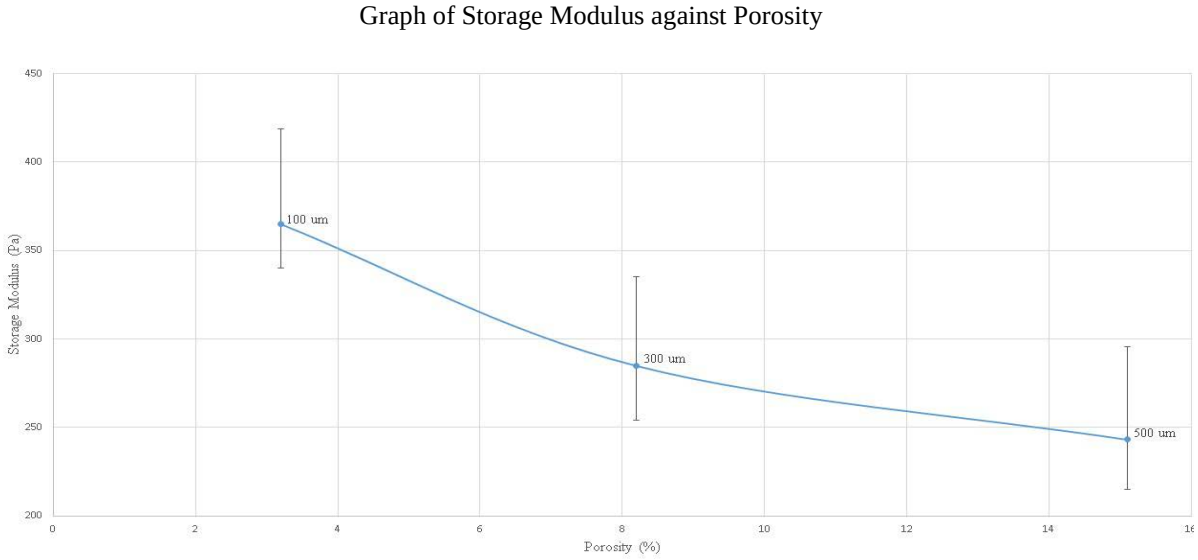

Figure 6. As the diameter of the microspheres are varied, the resulting porosity of the annealed gels are modified and can be related to changes in the storage modulus.

Annealed microspheres were also studied for the polymerization kinetics by quantifying the changes in storage modulus as the hydrogel network formed. Network formation is evident from the increase in storage modulus after UV exposure at 60 seconds (Figure 7). For each microsphere size, full networks were formed after 40 seconds of UV exposure. Following the same trends as shown earlier, as microsphere size increases, the bulk storage modulus increases. Comparing this to uniform hydrogels, there appears to be an uncommon initial storage modulus which is the result of the microspheres contributing to the initial gel stiffness.

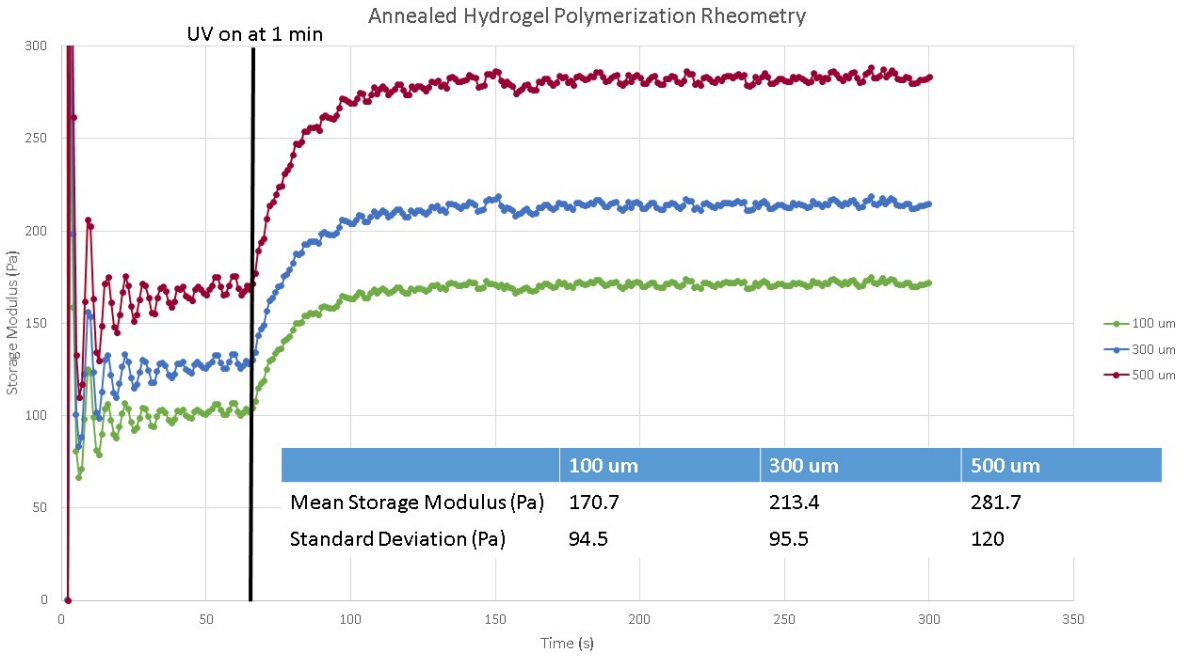

Figure 7. Network formation is evident from the change in gel stiffness when UV light is applied at one minute. Complete gel formation occurs at approximately 110 seconds for each microsphere diameter.

To understand the contribution of the microparticles to the overall gel stiffness, rheometry was conducted (Figure 8). Overall, the microspheres contribute to less than half of the gel stiffness for any given microsphere size, which means that total stiffness can be mostly attributed to the annealing process. By modifying the microsphere or the annealing solution, the stiffness can be controlled to a greater degree than in the traditional bulk hydrogels.

Graph of Mean Storage Modulus for Differing Microsphere Diameters

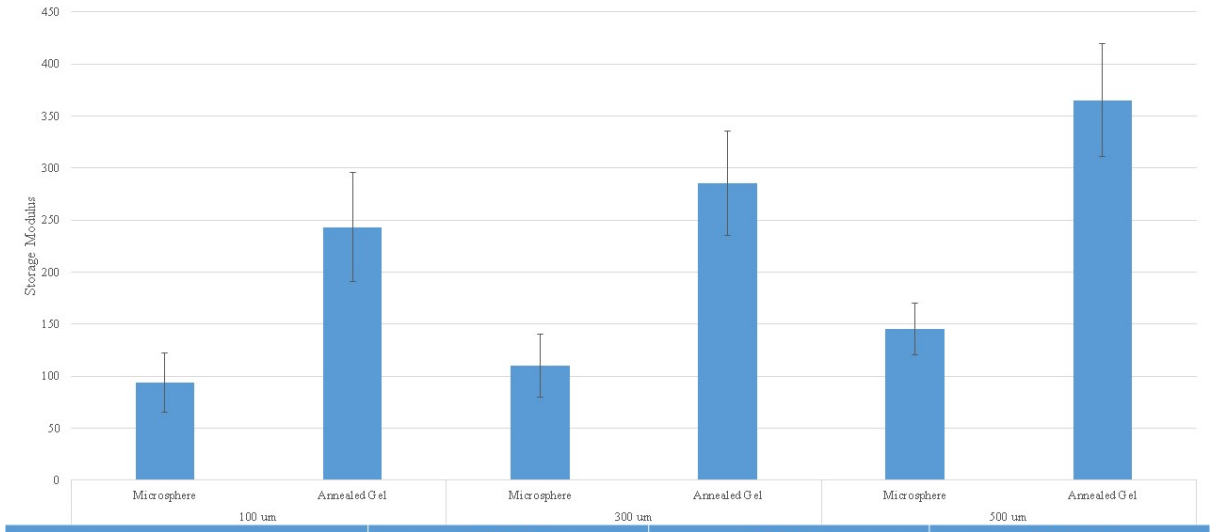

	100 um		300 um		500 um	
	Microsphere	Annealed Gel	Microsphere	Annealed Gel	Microsphere	Annealed Gel
Mean Storage Modulus (Pa)	94.1	243.2	110	284.9	145	364.9
Standard Deviation (Pa)	28.4	52.6	30.6	50.1	24.7	54.1

Figure 8. Microsphere stiffness does not comprise the majority of the annealed gel stiffness.

Endothelial cell invasion into the annealed gel

An important aspect of the wound healing process is revascularization of the synthetic matrix once it has been placed into the wound. Without proper vascularization, the chances for proper integration of the matrix diminish and any cell encapsulated within the matrix will die from improper nutrient exchange normally facilitated by the capillary network. In bulk hydrogels, vascularization is mediated by the incorporation of MMP-degradable linkers, which allow cells to create paths from which cells can migrate into. The process of creating a path through the matrix can generate a lot of stress on the cells which may contribute to the lower invasion when compared to natural ECM polymers such as collagen.

Figure 9 is a time-lapse image of the cellular infiltration of endothelial cells into an annealed microsphere matrix. In the images, it is shown that the endothelial cells are invading from the monolayer (shown in the bottom left corner) into the annealed microsphere gel.

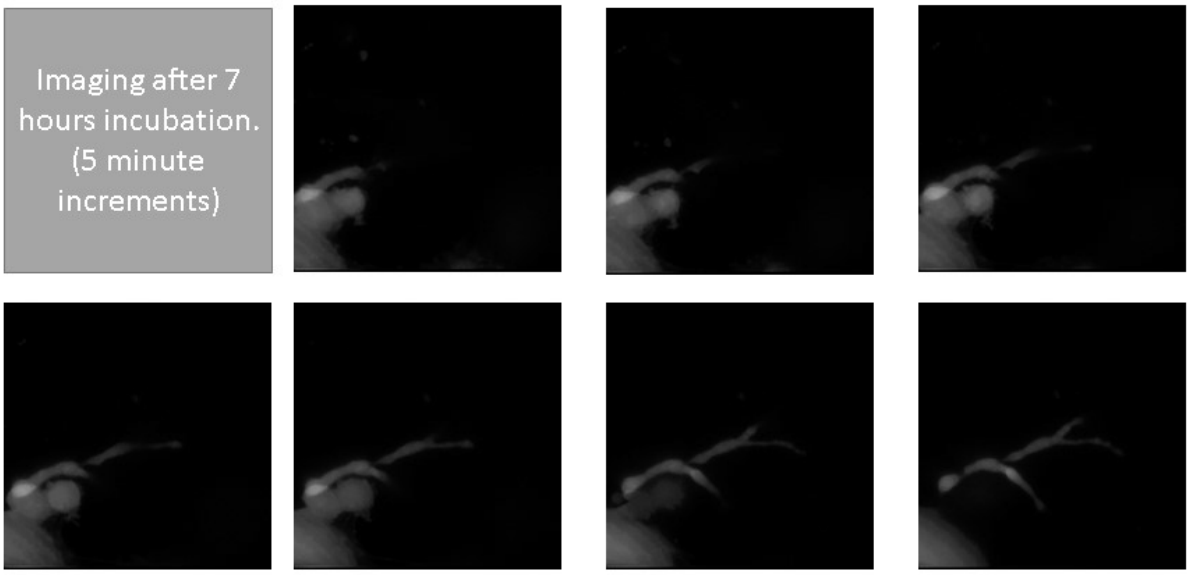

Figure 9. Cellular invasion into the annealed microsphere gel over the course of 35 minutes. Each image is taken five minutes apart.

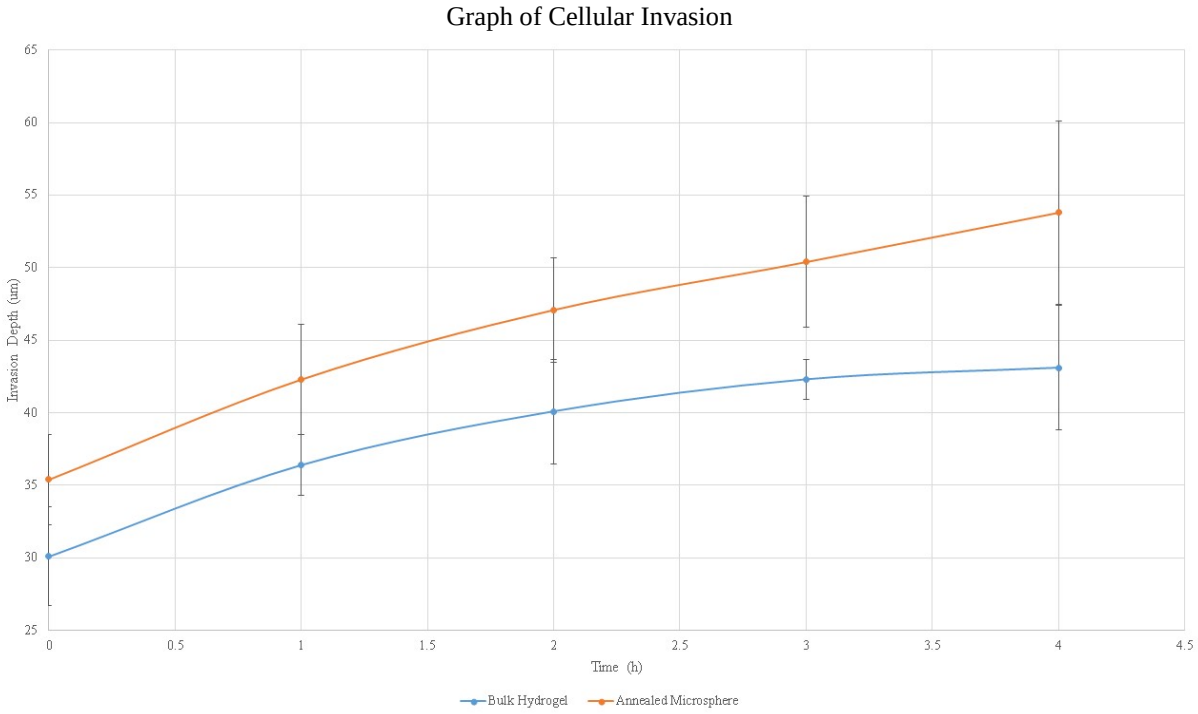

Figure 10. Cellular invasion into synthetic matrices. Invasion appears to move father into the annealed microsphere matrix as compared to the bulk hydrogel.

The invasion depth between the traditional bulk gel and annealed microspheres can be quantified over the course of 4 hours only after the initial incubation (Figure 10). No invasion depth data was collected during the initial 7-hour incubation period. The higher initial invasion depth of the annealed microparticles of about 35μm versus the 30μm of the bulk hydrogels possibly indicates the cells preference of the former over the latter. The invasion depth is normalized to the initial average depth of cells after the initial seven hours of incubation. Invasion depths for the bulk hydrogel was compared to annealed microspheres generated from 100 μm diameter spheres. The average invasion depth was further for the annealed microspheres with a fairly constant movement rate into the matrix. Compared to the bulk hydrogel, invasion does not seem to stagnate at the four hour mark. This can be attributed to multiple factors and requires further analysis to be understood properly.

CHAPTER IV

CONCLUSION

The wound healing process is a dynamic interaction between cells, bioactive factors and the extracellular environment. In this context, this paper has shown that microspheres of low polydispersity can be created very efficiently with a submerged electrospray system. Microspheres generated this way allow more control over stiffness, as manipulating their sphere sizes allows for the generation of varying levels of stiffness for the same thiol-ene ratio. In contrast, normal bulk hydrogels can only vary stiffness through stoichiometric adjustments. Initial endothelial cell invasions show that invasions into annealed microspheres are deeper than in their bulk hydrogel counterparts, however the invasion depth is still lacking compared to those that occur in collagen matrices. Figure 10 shows this data for the invasion depths of both the annealed microspheres and the bulk hydrogels.

In the future, an expansion on the cellular invasion model is needed in order to fully understand the relationship between porosity and cellular proliferation. Thus far, the paper has shown that stiffness levels of the electrospray microspheres are further correlated with sphere size by porosity, as increasing sphere sizes lead to lower porosity, thereby possibly decreasing cellular proliferation. This relationship is described by the data in Figure 6. Further research into this matter will therefore involve changing the diameter of the particles to vary porosity and then observing the resultant change in cellular proliferation. These results can also be quantified in terms of the varying stiffness levels.

REFERENCES

[1] B. D. Fairbanks, M.P. Schwartz, A.E. Halevi, C.R. Nuttleman, C.N. Bowman, K.S. Anset
A Versatile Synthetic Extracellular Matrix Mimic via Thiol-Norbornene Photopolymerization
Adv Mater, 21(2009), pp. 5005-5010

[2] M.P. Lutolf, J.A. Hubbell
Synthesis and physicochemical characterization of end-linked poly(ethylene glycol)-co-peptide hydrogels formed by michael-type addition
Biomacromolecules, 4 (2003), pp. 713–722

[3] K.A Kyburz, K.S Anseth
Three-dimensional hMSC motility within peptide-functionalized PEG-based hydrogels of varying adhesivity and crosslinking density
Acta Biomaterialia, 9(2013), pp. 6381-6392

[4] M.W. Tibbitt, K.S. Anseth
Hydrogels as extracellular matrix mimics for 3D cell culture
Biotechnol Bioeng, 103 (2009), pp. 655–663

[5] S.B Anderson, C.C. Lin, D.V. Kuntzler, K.S. Anseth
The performance of human mesenchymal stem cells encapsulated in cell-degradable polymer-peptide hydrogels
Biomaterials, 32(2011), pp. 3564-3574

[6] J.L. West, J.A. Hubbell
Polymeric biomaterials with degradation sites for proteases involved in cell migration
Macromolecules, 32 (1998), pp. 241–244

[7] M.P. Lutolf, J.L. Lauer-Fields, H.G. Schmoekel, A.T. Metters, F.E. Weber, G.B. Fields, *et al.*
Synthetic matrix metalloproteinase-sensitive hydrogels for the conduction of tissue regeneration: engineering cell-invasion characteristics
Proc Natl Acad Sci USA, 100 (2003), pp. 5413–5418

[8] P Carmeliet, R.K Jain
Angiogenesis in cancer and other diseases
Nature, 407(2000), pp. 249-257

[9] G. A. Di Lullo, S. M. Sweeney, J. Körkkö, L. Ala-Kokko, J.D. San Antonio,
Mapping the ligand-binding sites and disease-associated mutations on the most abundant protein in the human, type I collagen.
Journal of Biological Chemistry, *277*(2002), pp. 4223-4231

[10] D. Donovan, N.J. Brown, E.T. Bishop, C.E. Lewis
Comparison of three in vitro human 'angiogenesis' assays with capillaries formed in vivo
Angiogenesis, 4(2001), pp. 113-121

[11] K.J. Bayless, H. Kwak, S. Su
Investigating endothelial invasion and sprouting behavior in three-dimensional collagen matrices
Nature Protocols, 4(2009), pp. 1888-1898

[12] E. Ruoslahti
RGD and other Recognition Sequences for Integrins
Annu. Rev. Cell Dev. Biol., 12(1996), pp. 697-715

[13] D.G Stupack, D.A. Cheresh
Integrins and Angiogenesis
Curr. Topics in Dev. Biol., 64(2004), pp. 207-238

[14] D.R. Griffin, W.M. Weaver, P.O. Scumpia, D. D. Carlo, T. Segura
Accelerated wound healing by injectable microporous gel scaffolds assembled from annealed building blocks
Nature Materials, 14(2015), pp. 737-744

[15] H. Watanabe, H. Tanaka
A non-ionic surfactant as a new solvent for liquid—liquid extraction of zinc(II) with 1-(2-pyridylazo)-2-naphthol
Talanta, 25(1978), pp. 585-589

[16] A. Jaworek, A.T. Sobczyk
Electrospraying route to nanotechnology: An overview
Jour. Of Electrostatics, 66(2008), pp. 197-219

[17] C. J. Young, L. A. Poole-Warren, P.J. Martens
Combining Submerged Electrospray and UV Photopolymerization for Production of Synthetic Hydrogel Microspheres for Cell Encapsulation
Biotech. And Bioeng., 109(2012), pp. 1561-1570

APPENDIX A

Previous work has been done to discover scaling relationships between the sphere diameter to applied voltages and flow rates. In the most basic form, the diameter can be expressed purely as a function of the flow rate, given by equation 1.

$$\frac{d}{d_0} = b\left(\frac{Q}{Q_0}\right)^{1/3} \quad \textbf{Eqn. 1}$$

Where d is the diameter of the resultant sphere, Q is the applied flow rate, Q_0 is the characteristic value of flow rate, d_0 is the droplet diameter. To account for experimental variability, b is empirical scaling parameter dependent on the relationship between the viscosity of the polymer and the submerged liquid. The droplet diameter and characteristic value of flow rate can be expressed as described in equation 2 and equation 3:

$$Q_0 = \frac{\varepsilon_0 \gamma}{\rho K} \quad \textbf{Eqn. 2}$$

$$d_0 = \left(\frac{{\varepsilon_0}^2 \gamma}{\rho K^2}\right)^{1/3} \quad \textbf{Eqn. 3}$$

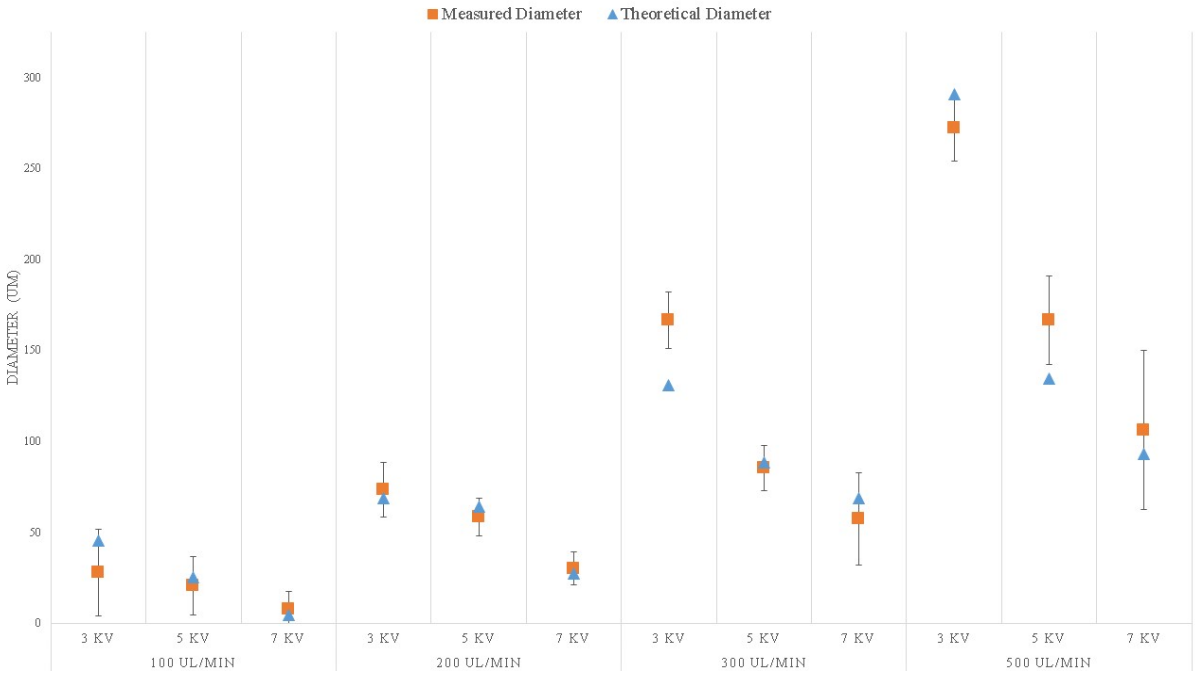

Figure 1. Comparison of theoretical and measured diameters for the submerged electrospray system.

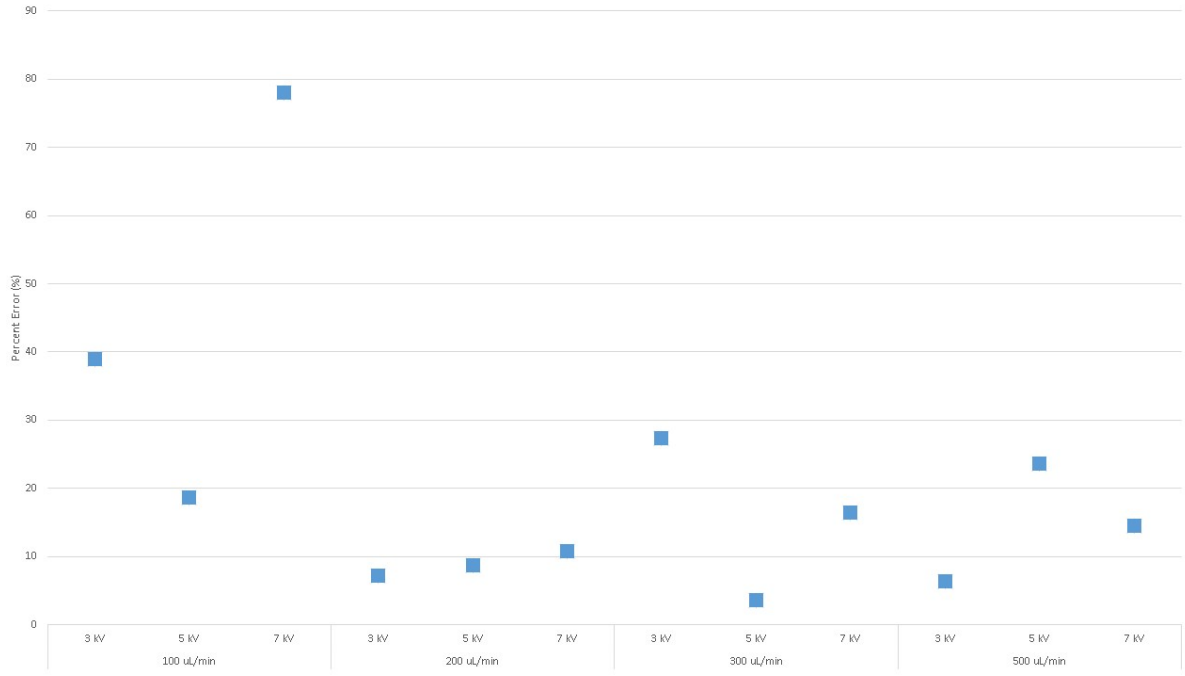

Figure 2. Percent Error between measured and theoretical diameters for given flow rates and voltages.

Here, Q_0 and d_0 can be described in terms of the vacuum permittivity constant (ε_0), surface tension (γ),density (ρ), and conductivity (K) of the polymer. These scaling laws can only be utilized under certain assumptions: 1) the viscosity of the polymer is much larger than the viscosity of the submerged liquid (in this case .5 wt% Span 80 in Mineral Oil), 2) the conductivity of the polymer is much higher than the submerged liquid, 3) the polymer is extruded from the needle tip at laminar flows.

To compare how good of a fit the mathematical model is to actual data, we compared the theoretical diameters to the measured values and computed the percent error between them (Figure 1 & Figure 2). Overall, the model is quite accurate. Because of the assumptions made to simply the scaling laws for this systems, the combinations of flow rate and voltage that produce a high deviation from the theoretical values must require the more complex expression for proper characterization.